Mapping of satellite derived surface albedo on the Mitdluagkat Glacier, Eastern Greenland, using a digital elevation model and SPOT HRV data

Anne Jacobsen, Allan R. Carstensen & John Kamper

Jacobsen, Anne, Allan R. Carstensen & John Kamper: Mapping of satellite derived surface albedo on the Mitdluagkat Glacier, Eastern Greenland, using a digital elevation model and SPOT HRV data. Geografisk Tidsskrift 93:6-18. Copenhagen 1993.

An approach for obtaining reflectance factors and surface albedo on a glaciated surface in a high relief environment combining a digital elevation model and SPOT HRV satellite data is presented. The methodology has been applied on the Mitdluagkat Glacier, Ammassalik, Eastern Greenland. Correction of reflectance factors with respect to solar incidence angle permits classification of different glacial metamorphic facies favourably compared with published data on field measurements from other glaciated regions. Development of surface albedo on reflectance factors corrected for solar incidence angle enables spatial analysis of the glaciated surface thus providing mapping of local climate induced surface features and the spatial distribution of ablation and accumulation zones on the Mitdluagkat Glacier.

Keywords: *glaciology, remote sensing, digital elevation model, mapping of surface albedo, mass balance.*

Anne Jacobsen, Allan R. Carstensen and John Kamper, Master students, Institute of Geography, University of Copenhagen, Øster Voldgade 10, DK-1350 Copenhagen K.

Satellite image processing is useful for studies of glaciers in remote high relief environments. Adequate estimation of satellite derived reflectance factors (Jones et al., 1988; Yang & Vidal, 1991) indicate the metamorphic state of the glacier (Dozier, 1989; Hall & Martinec, 1985; Hall et al., 1988, 1990) and additional knowledge of the spectral reflectance curve of snow and ice makes it possible to calculate the spatial surface albedo (Brest & Goward, 1987).

Mapping of surface albedo prospects mapping of the net solar radiation load on the glaciated surface and estimation of the spatial short wave radiation balance. Extrapolation of ground truth energy balance measurements through satellite data provides information on mass balance and potential run-off from the glacier - both important parameters to studies of the present state of a glacier and general climate change. Munro & Young (1990) find that solar net radiation is the most important parameter in glacial energy balances. Registered meltwater run-off measurements and its relation to spatial net solar radiation load calculated on satellite derived reflectance factors using a digital elevation model and a geographical information system has been evaluated in a recent investigation on the Mitdluagkat Glacier (Kamper et al., 1991). This paper concerns the calculation and glacial classification of the reflectance factors and the spatial analysis of the surface albedo maps estimated by Kamper et al. (1991).

STUDY AREA

The Mitdluagkat Glacier is located in a high relief mountainous environment in the subarctic zone at Ammassalik near the south-eastern coast of Greenland at 65°41' northern latitude and 37°48' western longitude (Fig. 1). The Mitdluagkat Glacier covers approximately 34 km^2 and the elevation is between 120 to 960 m a.s.l.. The main ablation zone is oriented towards west while the accumulation zone is oriented south-north. The glacier surface is dominantly facing northwest, west and southwest with the largest relative relief found in the accumulation zone.

Hydro-glaciological and climatological studies have been carried out successively on the Mitdluagkat Glacier since 1970. Mass balance has been positive from 1962 to 1980 (Hansen & Tastum, 1980; Hasholt, 1986) while the volume of the ablation zone has been decreasing from 1933 to 1970 (Fristrup, 1970) and from 1972 to 1981 (Hasholt, 1987).

DIGITAL ELEVATION MODEL

The basis of the digital elevation model is a topographical map scale 1:20.000 from 1981 of the Mitdluagkat Glacier produced from two series of air photographs from 1972 and 1981 (Hasholt, 1986, 1987). The map made covers the Mitdluagkat Glacier and a small non-glaciated area south of the glacier. The map covers 41.3 km^2 and the contour lines have 10 metre equidistance.

The map is digitalized along the contour lines and the resulting irregular digital (x,y,z) coordinates, have been grided into a regular grid net of cells each with an interpolated value of altitude estimated by the inverse distance quadrated weighted average method (Kamper et al., 1991). The digital elevation model thus produced contains 188 by 188 cells each representing (60 · 60) m^2 (Fig. 2).

The digital elevation model is transformed into a file format compatible with the applied geographical information system (GIS) for application of procedures incorporated in the GIS such as calculation of slope and aspect (Fig. 3) and spatial analysis of parameters derived from the digital elevation model and SPOT HRV data.

SPOT HRV DATA

The satellite image used in the present study is a high

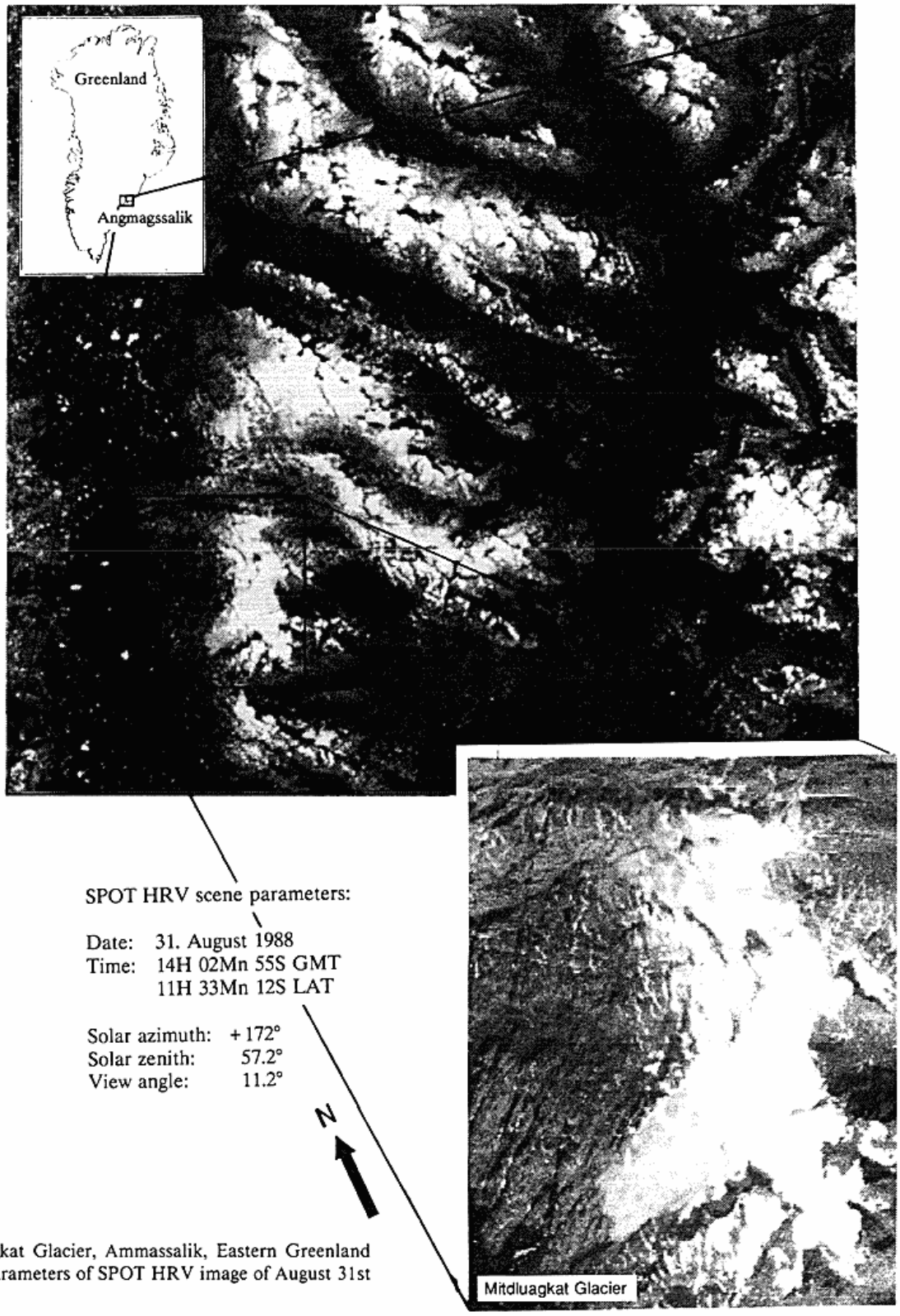

Fig. 1. Mitdluagkat Glacier, Ammassalik, Eastern Greenland and recording parameters of SPOT HRV image of August 31st 1988.

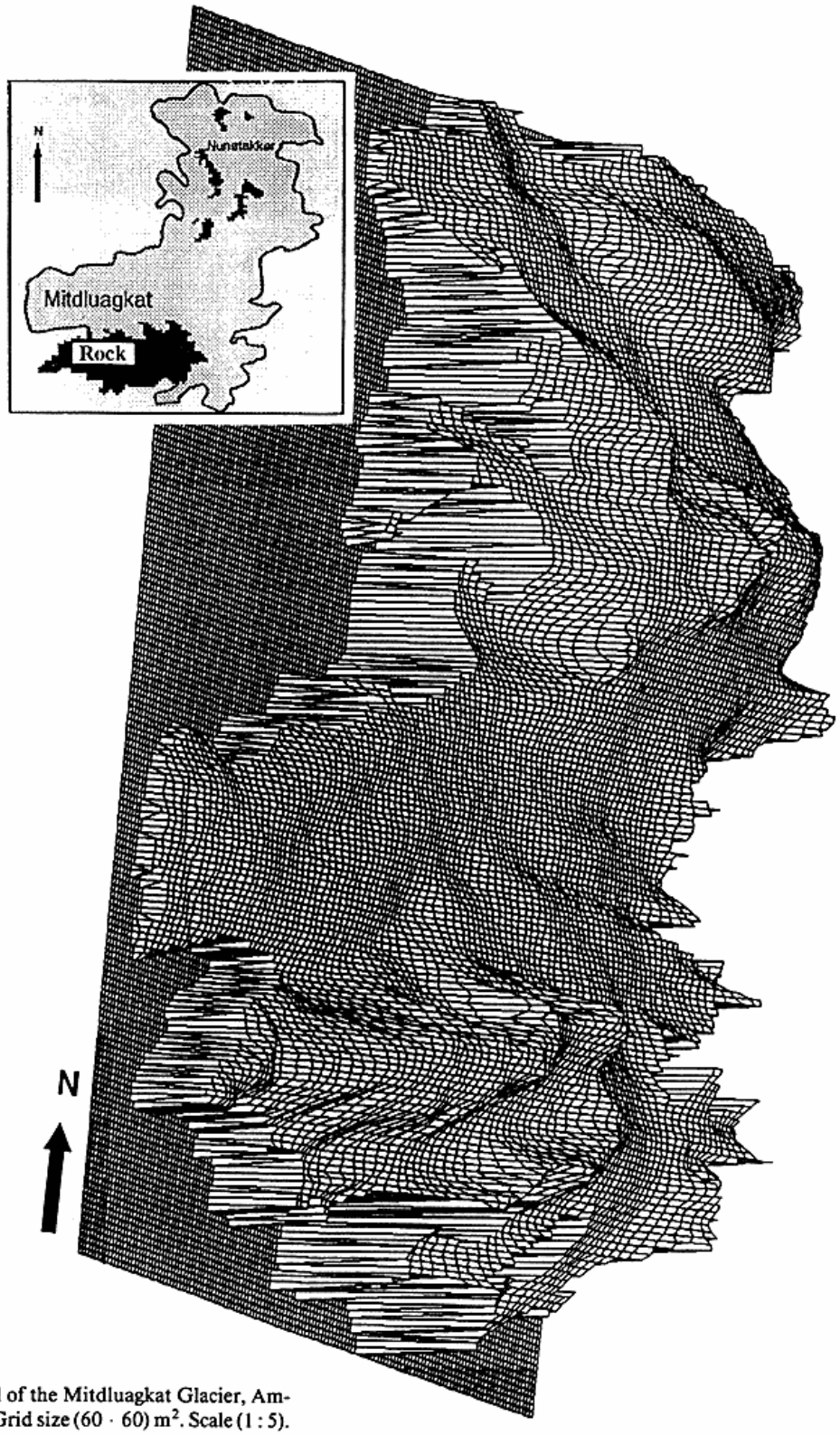

Fig. 2. Digital elevation model of the Mitdluagkat Glacier, Ammassalik, Eastern Greenland. Grid size (60 · 60) m^2. Scale (1 : 5).

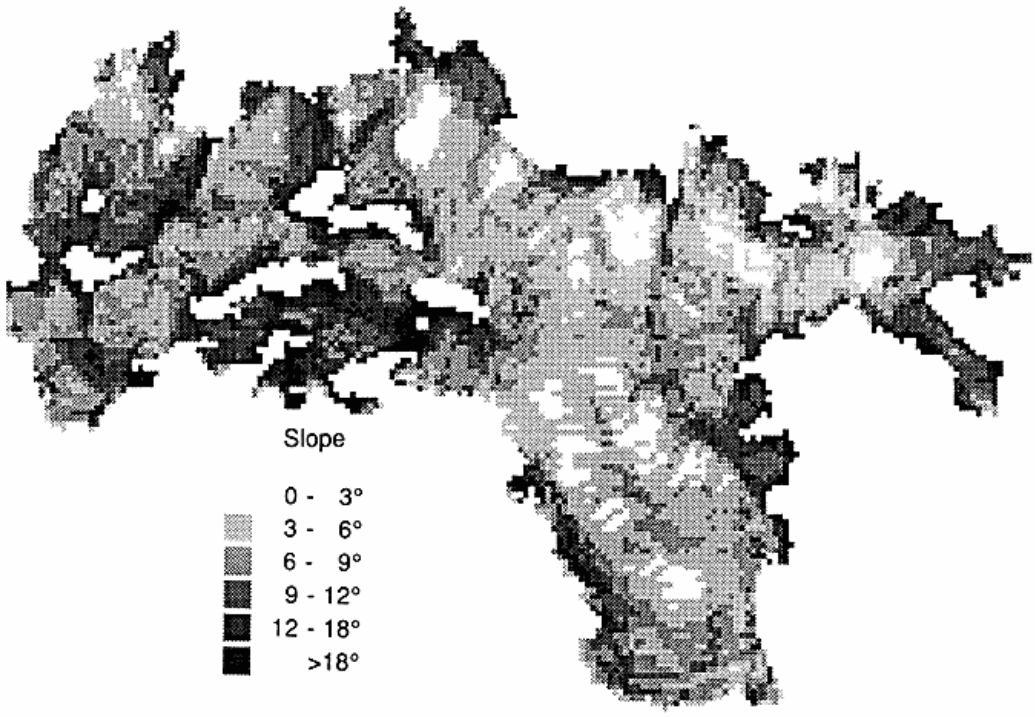

Fig. 3. Map of slope (top) and orientation (bottom) on Mitdluagkat Glacier derived from the digital elevation model in the geographical information system.

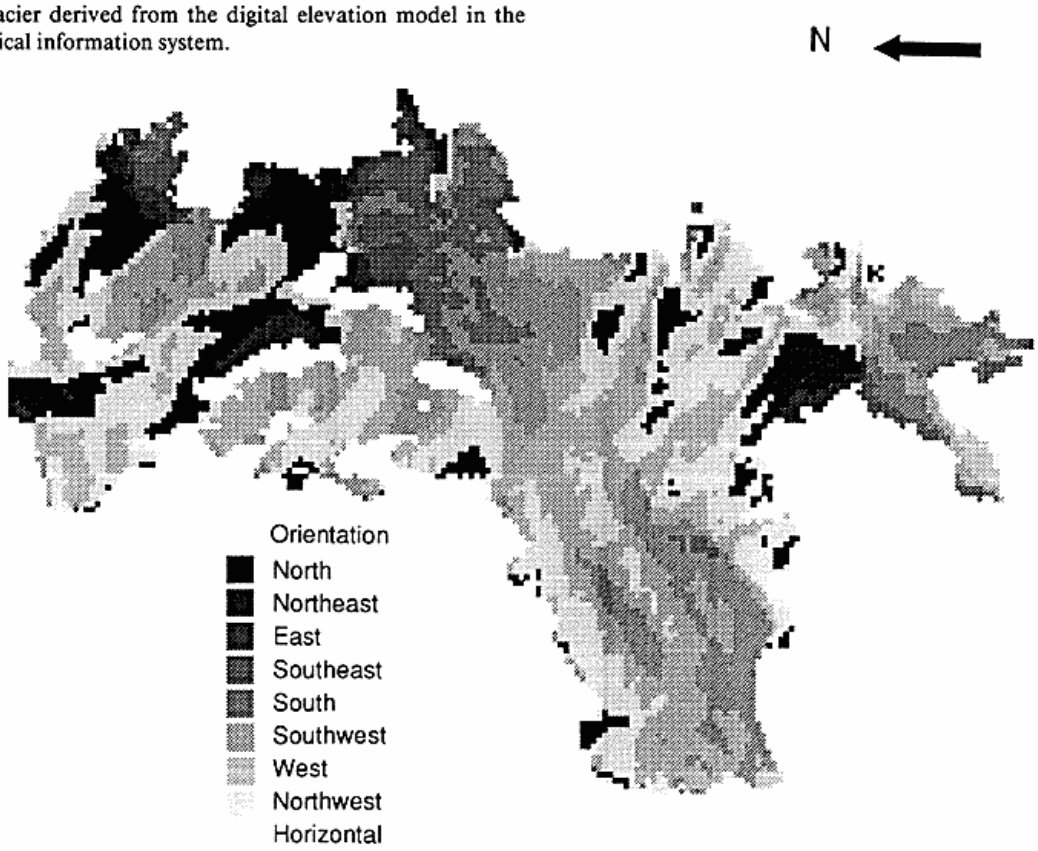

Sensorparameters	Sensor 1 0.50-0.59 µm	Sensor 2 0.61-0.68 µm	Sensor 3 0.79-0.89 µm
Gain W/m²srµm	0.81125	0.86078	0.97244
E_{exo} W/m²sr	586	504	331

Table 1. Sensorparameters of SPOT HRV August 31st 1988. Gain from image file header, spectral band width and equivalent exo-atmospheric solar irradiance (E_{exo}) from Price (1988).

resolution SPOT HRV image of resolution (20 · 20) m^2. SPOT HRV registrates with 3 sensors representing 2 spectral channels in the visible and 1 spectral channel in the near-infrared part of the solar electromagnetic spectrum (Table 1).

As differences in the metamorphic states of snow and ice may be recognized through the absolute and relative amount of reflectance in the visible and near-infrared wavelengths (Dozier, 1989), SPOT HRV offers possibilities for studies of glaciological importance of the best multispectral resolution possible.

The image chosen for the research is recorded on August 31st 1988 at the close of the mass balance year when seasonal snow is melted off the glacier and the new snow of the winter is yet to come. The satellite image is recorded on a clear day under cloudless conditions with a minimum of water vapour in the atmosphere to influence on the satellite signal. The image is thus providing the best terms for evaluation of the present state of the glacier (Fig. 1).

The satellite data are geometrically transformed to the map of the Mitdluagkat Glacier, the pixels of the resampled image being displaced less than 1.8 pixel (app. 35 m) in the (x,y) plane compared to the topographic map (Kamper et al., 1991).

The satellite image is filtrated by a smoothing filter for later resampling to obtain the resolution of the database, removing a few saturated pixels from the accumulation zone. The filter uses windows of 3 by 3 pixels to assign an average of the 9 pixels to the centre pixel later sampled accordingly reducing the resolution from (20 · 20) m^2 to (60 · 60) m^2, the image thus being transformed to the resolution of the database loosing only resolution and not information (Kamper et al., 1991).

METHODS

Interpreting satellite image registrations through reflectance factors requires knowledge of the total amount of irradiance received at the surface dependent on astronomical and atmospheric conditions at the time of the satellite overpass, the terrain relief and the reflectance properties of the surface.

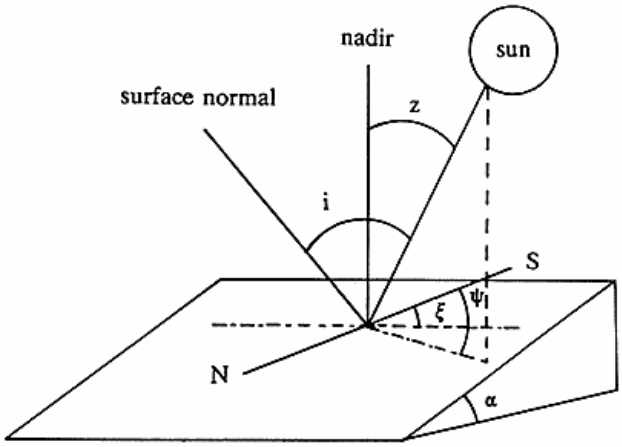

Fig. 4. Solar incidence angle (i) on an arbitrarily oriented surface depends on solar zenith angle (z), solar azimuth angle (ψ), and slope (α) and aspect (ξ) of the terrain.

Irradiance at the surface

The amount of direct, directional solar irradiation received on a horizontal surface (Si) is a function of the exo-atmospheric irradiance in a given spectral interval (E_{exo}, Table 1), the eccentricity ($(R0/R)^2$) and the length of the radiation path through the atmosphere as a function of zenith angle (z) (Iqbal, 1983):

$$Si = E_{exo} (R0/R)^2 \cos(z) \ (W/m^2sr) \qquad \text{(eq. 1)}$$

The direct irradiance flux received on an arbitrarily oriented surface is dependent of the solar incidence angle (Fig. 4).

The solar incidence angle (i) is a function of solar zenith (z) and azimuth (ψ) angles and the slope (α) and aspect (ξ) of the terrain with respect to south (Iqbal, 1983):

$$\cos(i) = (\cos(\alpha) \cos(z)) + (\sin(\alpha) \cos(\psi - \xi)) \qquad \text{(eq. 2)}$$

Solar zenith and azimuth angles are celestial unchanged over the area, the actual slope and orientation of the surface, however, highly variable, emphasizing the need of a digital elevation model to estimate the solar irradiance flux on the surface.

Cos(i) calculates the part of a unit area of a given terrain element actually exposed to the suns rays dependent of solar incidence angle. Accordingly, terrain elements exposed towards the sun receive a larger energy flux than terrain elements exposed away from the sun. On horizontal surfaces cos(i) is equal to cos(z). On surfaces with orientation app. 90° off solar azimuth the differences in cos(z) and cos(i) estimated irradiance flux is mainly due to the slope of the surface. On a gently undulated surface the

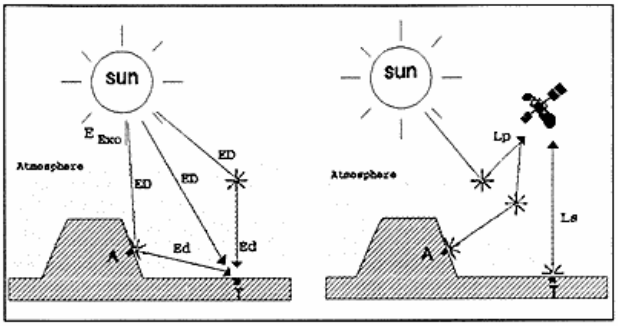

Fig. 5. The energy flux reaching the terrain target (T) originating from the exo-atmospheric solar irradiance (E_{exo}) is composed of direct irradiance (ED) and diffuse irradiance (Ed), the latter caused by atmospheric scattering and reflection from the adjacent terrain (A). The energy flux received at the satellite is composed of direct reflected radiance (Ls) from the terrain target (T) and path radiance (Lp) i.e. diffuse back-scattered radiance from the atmosphere and radiance reflected from the adjacent terrain (A).

difference in cos(z) and cos(i) estimated irradiance flux is thus small.

Diffuse irradiance on an arbitrarily oriented surface is composed of scattered radiation from the sky dependent on the sky view factor (the ratio of a hemisphere to the obstruction of the horizon by the terrain) and reflected radiation from the surrounding terrain to the pixel (Fig. 5). Diffuse irradiance is, however, very often estimated theoretically by means of the terrain view factor regarding the surrounding terrain as horizontal hence calculating the actual exposure of an arbitrarily oriented terrain element to an unobstructed sky hemisphere (Proy et al., 1989). The intensity of the diffuse irradiance from the sky to the pixel may be evaluated as isotropic or dependent on circum solar radiation and horizontal brightening (Temps & Coulsen, 1977).

Radiance at the satellite sensor

The reflected radiance received at the satellite is composed of direct and diffuse radiation reflected from the surface, backward scattering from the atmosphere and reflected radiation from other parts of the ground than the exact pixel, the latter two making up path radiance (Fig. 5) as an additional background radiance.

Reflected radiance is registered at the satellite as digital numbers (DN) from 0 to 255 representing minimum to maximum reflectance. DN is converted to spectral reflected radiance received at the satellite (Su) by multiplying DN with a sensorspecific gain (Table 1), (Price, 1987):

$$Su = DN/gain\ (W/m^2sr) \qquad \text{(eq. 3)}$$

Quantification of the attenuation of solar radiation on its way through the atmosphere and back to the satellite may be approached by evaluation of the correlation between solar incidence angle corrected direct irradiance, terrain view factor corrected diffuse radiance and path radiance through multiple regression analysis.

The methodology has been evaluated by Yang & Vidal (1991) over a forested area in southern France proving statistical significance assuming isotropic diffuse radiation. Dozier (1980) argues that diffuse radiation modelling should account for irradiance anisotropi over the sky hemisphere. In a high relief environment circum solar radiation should thus be included whereas horizontal brightening of the sky should be excluded. Kamper et al. (1991) find similar results on the Mitdluagkat Glacier and includes an expression of circum solar radiation in the regression analysis. The methodology proved, however, statistically insignificant on Mitdluagkat Glacier probably due to the fact that it leaves out of consideration the diffuse radiation reflected from the surrounding terrain to the actual pixel - an important parameter in a glacial environment.

Derivation of reflectance factors

Most natural surfaces including snow and ice are anisotropic reflectors reflecting radiance in different directions at different intensities as a function of the incidence angle of irradiance (Iqbal, 1983).

The satellite receives radiance reflected from the terrain target from one direction only (Fig. 5). The ratio of radiant flux reflected in a solid angle to radiant flux reflected in the same solid angle from a totally reflecting Lambertian surface (i.e. a surface reflecting all energy received at equal intensity in every direction) under identical irradiation is denoted the bidirectional reflectance factor (BRF) (Deering, 1989) commonly referred to as the reflectance factor (ρ). Assuming that the solar irradiance at the surface is the same as the solar radiance reflected in a given solid angle from a totally reflecting Lambertian surface, the ratio of satellite received radiance (outgoing radiance) to irradiance received at the surface (ingoing radiance) can be evaluated as the reflectance factor.

Accordingly, evaluation of eq. 1 and eq. 3 estimates the zenith angle reflectance factor ($\rho(z)$) accounting for the energy flux on a horizontal surface as a function of zenith angle and evaluation of eq. 1, eq. 2, and eq. 3 estimates the solar incidence angle reflectance factor ($\rho(i)$) accounting for the energy flux received on an arbitrarily oriented pixel as a function of solar incidence angle:

$$\rho(z) = (DN/gain)/((R0/R)^2 \cos(z)\ E_{exo}) \qquad \text{(eq. 4)}$$

$$\rho(i) = (DN/gain)/((R0/R)^2 \cos(i)\ E_{exo}) \qquad \text{(eq. 5)}$$

In a snow pack radiance mainly changes direction at interfaces between liquid and solid states whereas absorbtion takes place during the passage of crystals (Warren, 1982). The reflection and absorption of radiance is dependent on wavelength (Dozier, 1989). The effect of an increased snow grain size is an increased amount of absorbtion of the incoming solar radiation predominant in the infrared spectrum whereas debris in the snow-pack increases absorption predominant in the visible part of the spectrum where the absorption in the snow crystal is small.

As SPOT HRV channel 1 and 2 record in the visible part of the solar spectrum, reflectance factors of channel 1 and 2 enable evaluation of different amount of debris whereas reflectance factors of channel 3 in the near-infrared part of the solar spectrum make it possible to differentiate different metamorphic facies due to various grain sizes.

Derivation of surface albedo

Conversion from satellite derived reflectance factors of bidirectional reflectance to spectral albedo of hemispherical reflectance requires knowledge of the bidirectional distribution function (BRDF) (Deering, 1989). Assuming, however, Lambertian properties of the glacial surface neglecting increasing anisotropi as snow ages, reflectance factors may be evaluated as the spectral albedo and thus be used to estimate the solar surface albedo. Brest & Goward (1987) evaluate the solar surface albedo of different surfaces under dry atmospheric conditions by multiplying the reflectance factors of Landsat MSS channels by the proportional amount of solar radiation in a spectral interval representing the different channels. Kamper et al. (1991) uses the same principals of an average weighted scheme for SPOT HRV, referring the proportional solar radiation in visible, near and middle-infrared to channels 1, 2, and 3 of SPOT HRV (Fig. 6).

Accordingly, estimation of surface albedo is possible on SPOT HRV reflectance factors from channel 1, 2 and 3 (ρ_{CH1}, ρ_{CH2}, ρ_{CH3}) using weighting factors of figure 6 as multiplicative coefficients:

$$\text{albedo} = 0.526((\rho_{CH1} + \rho_{CH2})/2) + 0.232(\rho_{CH3}) + 0.130(0.63(\rho_{CH3}) + 0.112(0.065(\rho_{CH3}) \quad \text{(eq. 6)}$$

The coefficients 0.63 and 0.065 represent the ratio of the theoretical reflectance in segment 2 to segment 3 (0.63) and the ratio of theoretical reflectance in segment 2 to segment 4 (0.065) to overcome the fact that SPOT HRV only registrates in segment 1 and 2.

Albedo later referenced with suffix(z) or suffix(i) denotes albedo calculated on zenith angle reflectance factors (albedo(z)) and albedo calculated on incidence angle reflectance factors (albedo(i)).

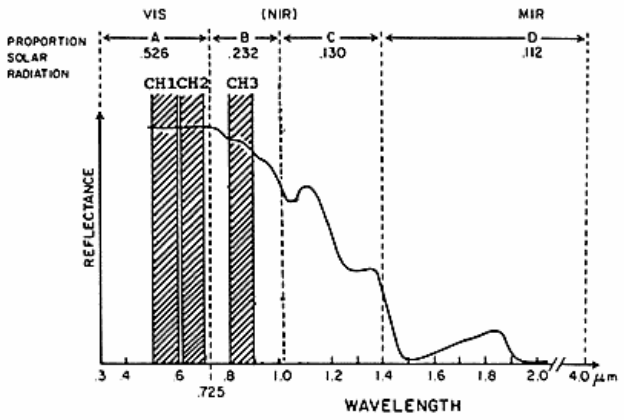

Fig. 6. Spectral reflectance curve of a snow-covered surface showing locations of SPOT HRV channels (CH1, CH2, CH3) and proportional amount of solar radiation in segment A, B, C, and D (adapted from Brest & Goward, 1987).

RESULTS AND DISCUSSION

To verify the influence of the terrain on the reflected radiance received at the satellite, a test area is chosen for statistical analysis of the correlation between solar incidence angle to the surface expressed by cos(i) and geometrically transformed raw satellite data (Table 2). To overcome the effect of increasing anisotropi of snow with increasing age, a homogeneous test area is chosen high in the accumulation zone where the snow cover probably has changed less due to metamorphosis.

The correlation coefficient (R) for channel 1, 2 and 3 show the same correlation for all three SPOT HRV channels indicating high dependency of cos(i) i.e. dependency of slope and orientation of the surface to the reflectance received at the satellite. Standard errors of estimate might partly be due to reflection anisotropi as standard error of estimate decreases with increasing wavelength, anisotropi being most distinct in shorter wavelengths (Warren, 1982).

Channel/regression parameters	Channel 1		Channel 2		Channel 3	
	coef.	std.	coef.	std.	coef.	std.
Cosi	139.1	3.17	139.3	3.06	89.12	2.03
Constant	105.9	1.83	84.80	1.79	60.64	1.17
Std.err. of est.	10.39		10.14		6.65	
Corr. coef. (R)	0.85		0.86		0.85	

Table 2. Linear regression analysis between cos(i) and geometrically transformed raw satellite data on a test area of 798 pixels (0.32 km^2) Mitdluagkat Glacier from SPOT HRV August 31st 1988.

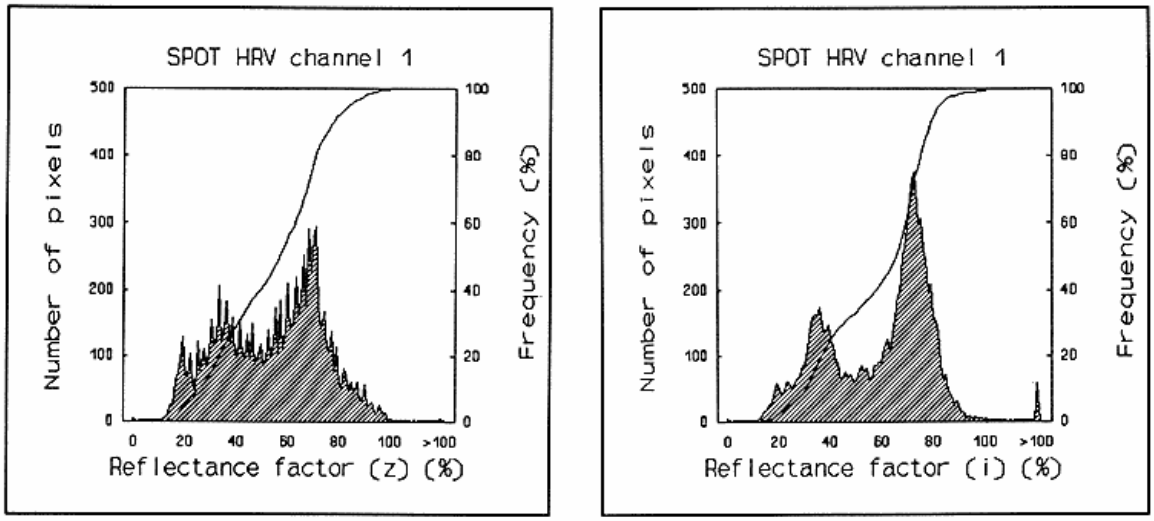

Fig. 7. Histograms and cummulated frequency of zenith angle reflectance factors (ρ(z)) and incidence angle reflectance factors (ρ(i)) on Mitdlaugkat Glacier from SPOT HRV channel 1 August 31st 1988.

SPOT HRV reflectance factors

Reflectance factors are calculated as zenith angle reflectance factors with respect to cos(z) (eq. 4) and as incidence angle reflectance factors with respect to cos(i) (eq. 5). The results are presented as histograms for channel 1 only (Fig. 7) as the results of channels 2 and 3 show the same features also evident through the discussion of table 2. The ρ(z) histogram is indented due to truncation not used in the further calculations.

The histogram shows that incidence angle correction of reflectance factors leads to a few estimates of ρ(i) up to and over 100 % i.e. the pixel is reflecting more radiance than it is actually receiving. Analysis finds that it concerns pixels with a cos(i) between 0.01 and 0.32. Proy et al. (1989) find the same effect on glaciated surfaces with cos(i) below 0.3 explaining it as due to a low estimated energy flux at the surface because of a small solar incidence angle compared to a high energy flux registered at the satellite because of additional reflection from the surrounding terrain to the satellite. 61 pixels on the glaciated surface on the Mitdluagkat Glacier has a cos(i) below 0.30 hence 7.5% of the incidence angle reflectance factor is estimated too high due to this effect.

The terrain effects on the reflectance factors become emphasized through the mean and standard deviations of the ablation and accumulation zones (Table 3).

ρ(z) has the largest standard deviation as the irradiance flux is corrected with the zenith angle estimating too little energy at pixels exposed towards the sun and too much energy at pixels exposed away from the sun. ρ(i) calculates the amount of energy as a function of incidence angle compensating for this effect reducing the standard deviation. The differences in standard deviation is largest in the accumulation zone due to a numeric larger reflectance and larger surface relief in this zone.

As the surface of the ablation zone to a larger extent than the surface of the accumulation zone is oriented towards the sun (Fig. 3) at the time of satellite image recording (solar azimuth 172°) ρ(i) mean is lower than ρ(z) mean in the ablation zone contrary to means in the accumulation zone.

Grain size and the amount of debris reflect metamorphic facies and classification of satellite derived reflectance factors can thus be used to estimate the ablation and accumulation zones of a glacier (Hall et al., 1988, 1990). The combination of large grain size and relatively large

	Channel 1		Channel 2		Channel 3	
Abl. zone	mean	std.	mean	std.	mean	std.
ρ(z)	33.10	4.8	31.21	4.9	28.31	4.5
ρ(i)	32.89	4.5	31.03	4.5	28.15	4.1
Acc. zone						
ρ(z)	72.92	8.9	70.56	9.4	62.73	8.8
ρ(i)	75.47	5.9	72.91	5.8	64.77	5.2

Table 3. Mean and standard deviation (std.) for zenith angle and incidence angle reflectance factors (ρ(z) and ρ(i)) of test areas in the ablation (abl.) and accumulation (acc.) zones of Mitdluagkat Glacier from SPOT HRV August 31st 1988.

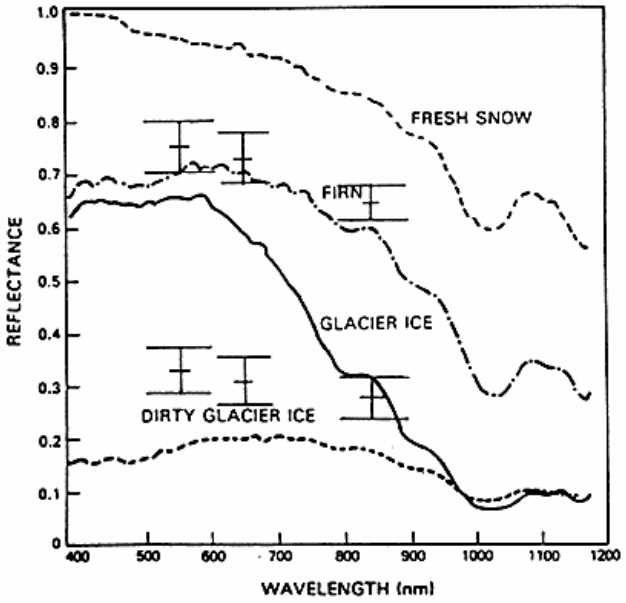

Fig. 8. Spectral reflectance curves of fresh snow, firn, glacier ice, and dirty glacier ice. Mean and standard deviation of incidence angle reflectance factors (ρ(i)) from SPOT HRV channel 1-3, August 31st 1988, are shown for the ablation and accumulation zones on the Mitdluagkat Glacier (adapted from Hall & Martinec, 1985).

amount of debris in the ablation zone causes low reflectance in all three SPOT channels whereas relatively small grain size and less debris in the accumulation zone causes high reflectance in channel 1 and 2 and lower reflectance in channel 3 (Fig. 8).

The classification of reflectance factors into two different classes of ablation and accumulation zones is evident through the mean and standard deviation of ρ(i) for SPOT HRV channel 1-3 plotted together with the spectral reflectance curves of snow and ice in different metamorphic facies (Fig. 8). Mean and standard deviation of channel 1, 2 and 3 of the accumulation zone show high reflectance in the visible wavelengths (channel 1 and 2) and a relative lower reflectance in the near-infrared (channel 3) corresponding to firn. Mean of channel 1, 2 and 3 of the ablation zone show the same level of reflectance in all three channels corresponding to dirty glacier ice.

Examples taken from literature on classification of reflectance factors on glaciers compare favourably to the results on the Mitdluagkat Glacier. On Meares Glacier in Alaska and on Gross Glockner Group in Austria Hall et al. (1988) find the same two distinct classes of reflectance factors. On basis of in situ measurements Hall et al. (1988) describe the low reflectance factors in the ablation zone (Mitdluagkat Glacier reflectance between 0.2 and 0.4,

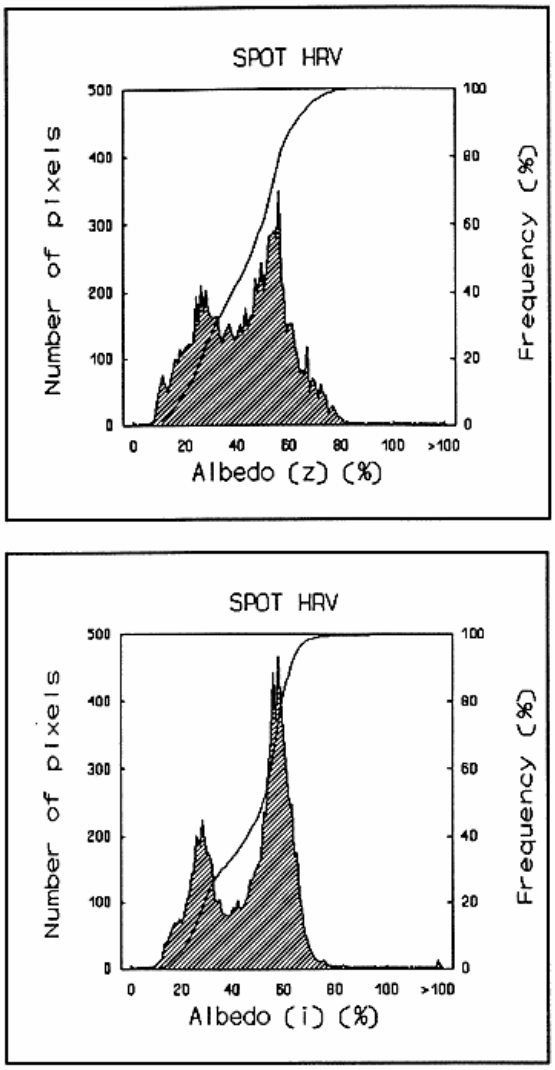

Fig. 9. Histograms and cummulated frequency of zenith angle albedo (albedo(z)) and incidence angle albedo (albedo(i)) on Mitdluagkat Glacier from SPOT HRV August 31st 1988. The bimodal distribution indicates the ablation zone (albedo ⟨ 40) and accumulation zone (albedo ⟩ 40).

Fig. 6) as being associated with pure ice, slush or debris covered ice and the higher reflectance factors in the accumulation zone (Mitdluagkat Glacier reflectance between 0.6 and 0.8, Fig. 6) as being associated with partly metamorphosed snow due to melting. The reflectance factors in the accumulation zone are lower in the visible wavelengths on the Gross Glockner Group than on Meares Glacier. This is due to a larger amount of impurities of atmospheric fall out in Austria causing lower reflectance

Abl. zone	mean	std.
Albedo(z)	26.01	4.0
Albedo(i)	25.85	3.6
Acc. zone		
Albedo(z)	57.87	7.6
Albedo(i)	59.87	4.7

Table 4. Mean and standard deviation (std.) of zenith angle and incidence angle albedo (albedo(z) and albedo(i)) of test areas in the ablation (abl.) and accumulation (acc.) zones of Mitdluagkat Glacier from SPOT HRV August 31st 1988.

especially in the shorter wavelengths. The reflectance factors of the Mitdluagkat Glacier in the Greenlandic arctic environment show the same effect, the reflectance in the accumulation zone being equivalent to reflectance registrated in the accumulation zone on Meares Glacier.

Surface albedo

As the estimation of surface albedo is based on an average weighted scheme between the three SPOT HRV channels (eq. 6) the ablation and accumulation zones are also distinct on the surface albedo shown by the bimodal distribution in the albedo histograms Fig. 9.

Mean and standard deviation of albedo(z) and albedo(i) from the two classes (Table 4) reveal analogue statistical analysis to the reflectance factors of the two classes. The terrain effects of the reflected solar radiation are thus similarly evident on the surface albedo.

An east-west longitudinal profile of the Mitdluagkat Glacier from the terminal glacier front to the bergschrund at the mountain ridge (Fig. 10) show the variation of albedo(z) and albedo(i) from the ablation zone over a transition zone to the accumulation zone.

The longitudinal profile shows the same general tendency of albedo(z) and albedo(i) variation with respect to horizontal distance from the glacier front and altitude asl. The differences between albedo(z) and albedo(i) discussed through Table 4 and 5 are thus locally induced due to undulations of the glacier surface later confirmed by the spatial analysis.

Spatial analysis of surface albedo

Analysis in the geographical information system confirms the distribution of differences in albedo(z) and albedo(i) caused by slope and orientation of the surface as indicated by the definition of cos(i) (eq. 2). Albedo(i) is higher than albedo(z) on pixels with a northern orientation compared to pixels with a southern orientation as solar azimuth of 172° at the time of satellite recording causes a higher energy flux at pixels exposed against the sun than at pixels exposed away from the sun (Fig. 11). According to eq. 2

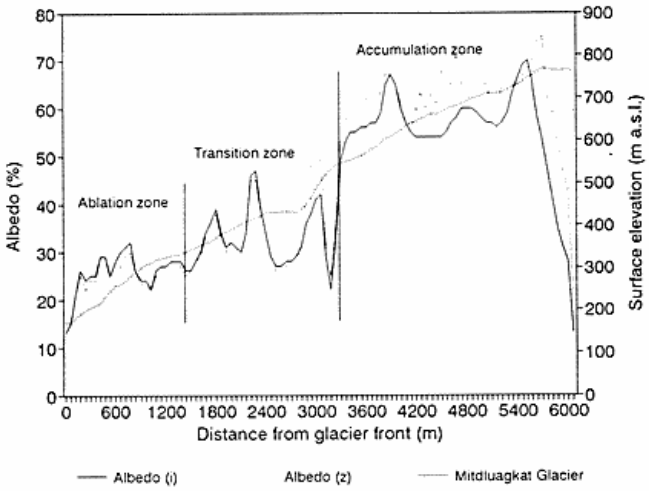

Fig. 10. Longitudinal profile of the Mitdluagkat Glacier showing the variation of albedo(z) and albedo(i) from the glacier front to the bergschrund. The cross section indicates the location of ablation, transition, and accumulation zones. The pronounced decrease in albedo at the beginning and end of the profile is caused by reflection from the surrounding non glaciated area. Scale (1 : 5).

the turning point is +/- 90° off solar azimuth where the surface changes between facing the sun and being exposed away from the sun.

Interpretation of zenith angle albedo (albedo(z)) and incidence angle albedo (albedo(i)) maps (Fig. 12) show the effect on spatial analysis of surface characteristics of the Mitdluagkat Glacier using the two different methods to derive reflectance factors hence albedo.

Location of ablation zones in the lower parts of the glacier arms is not influenced by terrain effects. The abla-

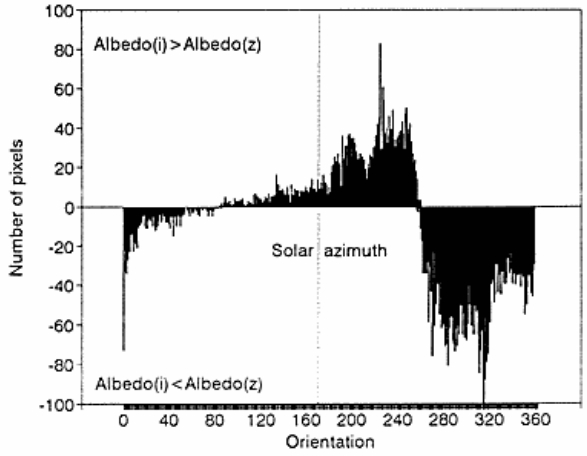

Fig. 11. Histogram of number of pixels with albedo(i) ⟩ albedo(z) (positive values) and albedo(i) ⟨ albedo(z) (negative values) with respect to orientation. Solar azimuth 172°.

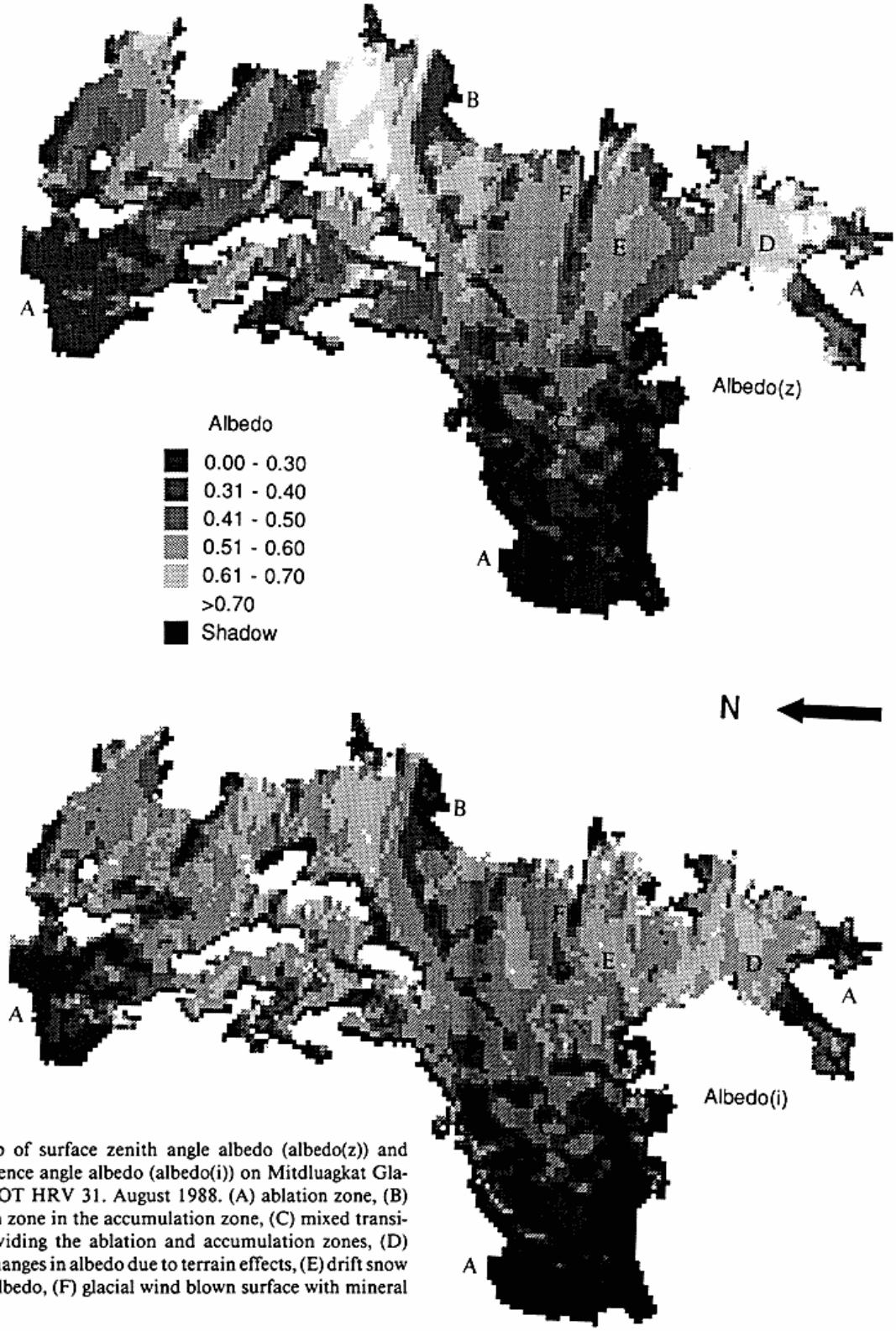

Fig. 12. Map of surface zenith angle albedo (albedo(z)) and surface incidence angle albedo (albedo(i)) on Mitdluagkat Glacier from SPOT HRV 31. August 1988. (A) ablation zone, (B) local ablation zone in the accumulation zone, (C) mixed transition zone dividing the ablation and accumulation zones, (D) example of changes in albedo due to terrain effects, (E) drift snow with a high albedo, (F) glacial wind blown surface with mineral dust.

tion zone (A) is located app. below 500 m a.s.l. on the main glacier tongue, below 500 m a.s.l. on the northern tongues and below app. 700 m a.s.l. on the southern tongues. The difference in elevation is due to the local climate being less severe at the southern arms evidenced by the equilibrium line altitude (ELA) at app. 400 m a.s.l. whereas the ELA at the main and northern glacier arms are at app. 200 m a.s.l..

Incidence angle albedo reveals a local ablation area (B) in the accumulation zone. In this area the glacier is oriented against east and terminal moraines found in front of this area verifies the classification. The area of low reflectance stretches further west into the accumulation zone and is also recognized on air photos from 1972. This area is penetrated by glacier crevasses resulting in a larger specific surface causing irradiance to penetrate into the snow pack and reemerge as diffuse radiation instead of being reflected directly to the satellite.

A broad mixed zone is dividing the ablation and accumulation zones (C). The differences in albedo in the area is not affected by the incidence angle correction the areas with the highest albedo being due to a large amount of drift snow accumulated behind the icefall in the winter.

The saddle shaped glacier divide in the southern part of the accumulation zone (D) shows how high albedo on southern parts and low albedo on northern parts are removed using the incidence angle method. Instead an area of high albedo (E) is revealed on the northernmost part of the glacier divide caused by accumulation of drift snow behind the mountain ridge. The dark area on the northernmost part of the glacier divide is not completely removed emphasizing an area dominated by mineral dust on a glacial wind blown surface (F). Field investigations in the summer of 1988 by Ole Humlum verifies the classification.

CONCLUSION

Regression analysis on incidence angle reflectance factors show a high correlation between DN and cos(i) in the three SPOT HRV channels. The resemblance between reflectance factors and glacial reflectance curves enables classification of the reflectance factor into two distinct glacial surfaces representing the ablation and accumulation zones. Incidence angle reflectance factors improve classification overestimating, however, pixels with a cos(i) below 0.3. Spatial analysis of the glacier based on albedo maps estimated on incidence angle reflectance factors reveals important characteristics of the glacier surface otherwise blurred by terrain effects.

SUMMARY

In this paper two methods for estimating reflectance factors from SPOT HRV data over a rugged glaciated surface are presented. Reflectance factors are estimated with respect to zenith angle corrected solar irradiance and incidence angle corrected solar irradiance i.e. is with respect to slope and aspect of the terrain.

The results show reasonable accordance with other investigations of glaciated areas based on in situ measurement and the incident angle reflectance factor improves the classification of different metamorphic facies on the glacier. Remotely sensed data can be used to map surface albedo and mapping of surface albedo calculated on an average weighted scheme based on incidence angle reflectance factors improves spatial analysis of the metamorphic facies on the glacier. Incidence angle correction removes the influence on the satellite derived signal due to the high relief environment and the research accordingly emphasizes the importance of a digital elevation model to satellite image interpretation.

The methodology prospects mapping of net solar radiation through incidence angle surface albedo and the high spatial resolution offered by SPOT HRV and permanent registration of run-off measurements will undoubtedly reveal important knowledge of the glacio-hydrological properties of the Mitdluagkat Glacier.

ACKNOWLEDGEMENTS

The authors are grateful to Birger Hansen, Ole Humlum, and Bent Hasholt for contribution of data used in this research and interesting discussions.

References

Brest, Christopher L., & Goward, Samuel N. (1987): Deriving Surface Albedo Measurements from Narrow Band Satellite Data. International Journal of Remote Sensing, 1987, vol. 8, no. 3, pp. 351-367.

Dechamps, P. Y., Herman, M. & Tanre, D. (1983): Definitions of Atmospheric Radiance and Transmittance in Remote Sensing. Short Communication. Remote Sensing of Environment, 1983, vol. 13, pp. 89-92.

Deering, D. W. (1989): Field Measurements of Bidirectional Reflectance. Theory and Applications of Optical Remote Sensing, edt. Asrar, G., 1989, pp. 14-21.

Dozier, Jeff (1980): A Clear-Sky Spectral Solar Radiation Model for Snow-Covered Mountainous Terrain. Water Resources Research, 1980, vol. 16, no. 4, pp. 709-718.

Dozier, Jeff (1989): Remote Sensing of Snow in Visible and Near-Infrared Wavelengths. Theory and Applications of Optical Remote Sensing, edt. Asrar, G., 1989, pp. 527-547.

Fristrup, Børge (1970): Ny geografisk station i Grønland. Geografisk Tidsskrift, 1970, bind 69, pp. 192-203.

Hall & Martinec (1985): Remote Sensing of Ice and Snow. University Press, Cambridge.

tion zone (A) is located app. below 500 m a.s.l. on the main glacier tongue, below 500 m a.s.l. on the northern tongues and below app. 700 m a.s.l. on the southern tongues. The difference in elevation is due to the local climate being less severe at the southern arms evidenced by the equilibrium line altitude (ELA) at app. 400 m a.s.l. whereas the ELA at the main and northern glacier arms are at app. 200 m a.s.l..

Incidence angle albedo reveals a local ablation area (B) in the accumulation zone. In this area the glacier is oriented against east and terminal moraines found in front of this area verifies the classification. The area of low reflectance stretches further west into the accumulation zone and is also recognized on air photos from 1972. This area is penetrated by glacier crevasses resulting in a larger specific surface causing irradiance to penetrate into the snow pack and reemerge as diffuse radiation instead of being reflected directly to the satellite.

A broad mixed zone is dividing the ablation and accumulation zones (C). The differences in albedo in the area is not affected by the incidence angle correction the areas with the highest albedo being due to a large amount of drift snow accumulated behind the icefall in the winter.

The saddle shaped glacier divide in the southern part of the accumulation zone (D) shows how high albedo on southern parts and low albedo on northern parts are removed using the incidence angle method. Instead an area of high albedo (E) is revealed on the northernmost part of the glacier divide caused by accumulation of drift snow behind the mountain ridge. The dark area on the northernmost part of the glacier divide is not completely removed emphasizing an area dominated by mineral dust on a glacial wind blown surface (F). Field investigations in the summer of 1988 by Ole Humlum verifies the classification.

CONCLUSION

Regression analysis on incidence angle reflectance factors show a high correlation between DN and cos(i) in the three SPOT HRV channels. The resemblance between reflectance factors and glacial reflectance curves enables classification of the reflectance factor into two distinct glacial surfaces representing the ablation and accumulation zones. Incidence angle reflectance factors improve classification overestimating, however, pixels with a cos(i) below 0.3. Spatial analysis of the glacier based on albedo maps estimated on incidence angle reflectance factors reveals important characteristics of the glacier surface otherwise blurred by terrain effects.

SUMMARY

In this paper two methods for estimating reflectance factors from SPOT HRV data over a rugged glaciated surface are presented. Reflectance factors are estimated with respect to zenith angle corrected solar irradiance and incidence angle corrected solar irradiance i.e. is with respect to slope and aspect of the terrain.

The results show reasonable accordance with other investigations of glaciated areas based on in situ measurement and the incident angle reflectance factor improves the classification of different metamorphic facies on the glacier. Remotely sensed data can be used to map surface albedo and mapping of surface albedo calculated on an average weighted scheme based on incidence angle reflectance factors improves spatial analysis of the metamorphic facies on the glacier. Incidence angle correction removes the influence on the satellite derived signal due to the high relief environment and the research accordingly emphasizes the importance of a digital elevation model to satellite image interpretation.

The methodology prospects mapping of net solar radiation through incidence angle surface albedo and the high spatial resolution offered by SPOT HRV and permanent registration of run-off measurements will undoubtedly reveal important knowledge of the glacio-hydrological properties of the Mitdluagkat Glacier.

ACKNOWLEDGEMENTS

The authors are grateful to Birger Hansen, Ole Humlum, and Bent Hasholt for contribution of data used in this research and interesting discussions.

References

Brest, Christopher L., & Goward, Samuel N. (1987): Deriving Surface Albedo Measurements from Narrow Band Satellite Data. International Journal of Remote Sensing, 1987, vol. 8, no. 3, pp. 351-367.

Dechamps, P. Y., Herman, M. & Tanre, D. (1983): Definitions of Atmospheric Radiance and Transmittance in Remote Sensing. Short Communication. Remote Sensing of Environment, 1983, vol. 13, pp. 89-92.

Deering, D. W. (1989): Field Measurements of Bidirectional Reflectance. Theory and Applications of Optical Remote Sensing, edt. Asrar, G., 1989, pp. 14-21.

Dozier, Jeff (1980): A Clear-Sky Spectral Solar Radiation Model for Snow-Covered Mountainous Terrain. Water Resources Research, 1980, vol. 16, no. 4, pp. 709-718.

Dozier, Jeff (1989): Remote Sensing of Snow in Visible and Near-Infrared Wavelengths. Theory and Applications of Optical Remote Sensing, edt. Asrar, G., 1989, pp. 527-547.

Fristrup, Børge (1970): Ny geografisk station i Grønland. Geografisk Tidsskrift, 1970, bind 69, pp. 192-203.

Hall & Martinec (1985): Remote Sensing of Ice and Snow. University Press, Cambridge.

Hall, Dorothy K., Chang, Alfred T. C. & Siddalingaiah, H. (1988): Reflectances of Glaciers as Calculated Using Landsat-5 Thematic Mapper Data. Remote Sensing of Environment, 1988, vol. 25, pp. 311-321.

Hall, Dorothy K., Bindschadler, R. A., Foster, J. L., Chang, A. T. C. & Siddalingaiah, H. (1990): Comparison of In Situ and Satellite-derived Reflectances of Forbindels Glacier, Greenland. International Journal of Remote Sensing, 1990, vol. 11, no. 3, pp. 493-504.

Hansen, B. & Tastum, J. (1980): Sermilik 1979. Institute of Geography, University of Copenhagen. Unpubl. internal report.

Hasholt, Bent (1986): Mapping of the Mitdluagkat Glacier and some hydro-glaciological observations. Geografisk Tidsskrift, vol. 86, pp. 9-19, 1986.

Hasholt, Bent (1987): A New Map of the Mitdluagkat Glacier - a preliminary report. Geografisk Tidsskrift, vol. 87, pp. 19-22, 1987.

Hasholt, Bent (1988): Mass Balance Studies of the Mitdluagkat Glacier, Eastern Greenland. Geografisk Tidsskrift, vol. 88, pp. 82-85, 1988.

Iqbal, Muhammad (1983): An Introduction to Solar Radiation. Academic Press, 1983.

Jones, A. R., Settle, J. J. & Wyatt, B. K. (1988): Use of digital terrain data in the interpretation of SPOT-1 HRV multispectral imagery. International Journal of Remote Sensing, vol. 9, no. 4, pp. 669-682, 1988.

Kamper, John, Jacobsen, Anne & Carstensen, Allan R. (1991): Normalisering af satellitregistreret reflektans fra en glacial overflade, rumlig analyse af BRF og albedo samt afsmeltningsmodellering i et geografisk informationssystem. Institute of Geography, University of Copenhagen. Unpubl. internal report.

Munro, D. S. & Young, G. J. (1982): An Operational Net Shortwave Radiation Model for Glacier Basins. Water Resources Research, 1982, vol. 18, no. 2, pp. 220-231.

Price, John C. (1987): Calibration of Satellite Radiometers and the Comparison of Vegetation Indices. Remote Sensing of Environment, 1987, vol. 21, pp. 15-27.

Price, John C. (1988): An Update on Visible and Near Infrared Calibration of Satellite Instruments. Remote sensing of Environment, 1988, vol. 24, pp. 419-422.

Proy, C., Tanre, D. & Dechamps, P. Y. (1989): Evaluation of Topografic Effects in Remotely Sensed Data. Remote Sensing of Environment, 1989, vol. 30, pp. 21-32.

Temps, Ralph C. & Coulson, K. L. (1977): Solar Radiation Incident upon Slopes of Different Orientation. Solar Energy, 1977, vol. 19, no. 2, pp. 179-184.

Valeur, Hans (1959): Runoff Studies from the Mitdluagkat Gletscher in SE-Greenland during the Late Summer 1958. Geografisk Tidsskrift, 1959, bind 58, pp. 54-65.

Warren, Stephen G. (1982): Optical Properties of Snow. Reviews of Geophysics and Space Physics, 1982, vol. 20, no. 1, pp. 67-89.

Woodham, J. R. & Gray, Malcolm H. (1987): An Analytic Method for Radiometric Correction of Satellite Multispectral Scanner Data. IEEE Transactions on Geoscience and Remote Sensing, 1987, vol. GE-25, pp. 258-271.

Yang, Chogun & Vidal, Alain (1990): Combination of Digital Elevation Models with SPOT-1 HRV Multispectral Imagery for Reflectance Factor Mapping. Remote Sensing of Environment, 1990, vol. 32, pp. 35-45.

tion zone (A) is located app. below 500 m a.s.l. on the main glacier tongue, below 500 m a.s.l. on the northern tongues and below app. 700 m a.s.l. on the southern tongues. The difference in elevation is due to the local climate being less severe at the southern arms evidenced by the equilibrium line altitude (ELA) at app. 400 m a.s.l. whereas the ELA at the main and northern glacier arms are at app. 200 m a.s.l..

Incidence angle albedo reveals a local ablation area (B) in the accumulation zone. In this area the glacier is oriented against east and terminal moraines found in front of this area verifies the classification. The area of low reflectance stretches further west into the accumulation zone and is also recognized on air photos from 1972. This area is penetrated by glacier crevasses resulting in a larger specific surface causing irradiance to penetrate into the snow pack and reemerge as diffuse radiation instead of being reflected directly to the satellite.

A broad mixed zone is dividing the ablation and accumulation zones (C). The differences in albedo in the area is not affected by the incidence angle correction the areas with the highest albedo being due to a large amount of drift snow accumulated behind the icefall in the winter.

The saddle shaped glacier divide in the southern part of the accumulation zone (D) shows how high albedo on southern parts and low albedo on northern parts are removed using the incidence angle method. Instead an area of high albedo (E) is revealed on the northernmost part of the glacier divide caused by accumulation of drift snow behind the mountain ridge. The dark area on the northernmost part of the glacier divide is not completely removed emphasizing an area dominated by mineral dust on a glacial wind blown surface (F). Field investigations in the summer of 1988 by Ole Humlum verifies the classification.

CONCLUSION

Regression analysis on incidence angle reflectance factors show a high correlation between DN and cos(i) in the three SPOT HRV channels. The resemblance between reflectance factors and glacial reflectance curves enables classification of the reflectance factor into two distinct glacial surfaces representing the ablation and accumulation zones. Incidence angle reflectance factors improve classification overestimating, however, pixels with a cos(i) below 0.3. Spatial analysis of the glacier based on albedo maps estimated on incidence angle reflectance factors reveals important characteristics of the glacier surface otherwise blurred by terrain effects.

SUMMARY

In this paper two methods for estimating reflectance factors from SPOT HRV data over a rugged glaciated surface are presented. Reflectance factors are estimated with respect to zenith angle corrected solar irradiance and incidence angle corrected solar irradiance i.e. is with respect to slope and aspect of the terrain.

The results show reasonable accordance with other investigations of glaciated areas based on in situ measurement and the incident angle reflectance factor improves the classification of different metamorphic facies on the glacier. Remotely sensed data can be used to map surface albedo and mapping of surface albedo calculated on an average weighted scheme based on incidence angle reflectance factors improves spatial analysis of the metamorphic facies on the glacier. Incidence angle correction removes the influence on the satellite derived signal due to the high relief environment and the research accordingly emphasizes the importance of a digital elevation model to satellite image interpretation.

The methodology prospects mapping of net solar radiation through incidence angle surface albedo and the high spatial resolution offered by SPOT HRV and permanent registration of run-off measurements will undoubtedly reveal important knowledge of the glacio-hydrological properties of the Mitdluagkat Glacier.

ACKNOWLEDGEMENTS

The authors are grateful to Birger Hansen, Ole Humlum, and Bent Hasholt for contribution of data used in this research and interesting discussions.

References

Brest, Christopher L., & Goward, Samuel N. (1987): Deriving Surface Albedo Measurements from Narrow Band Satellite Data. International Journal of Remote Sensing, 1987, vol. 8, no. 3, pp. 351-367.

Dechamps, P. Y., Herman, M. & Tanre, D. (1983): Definitions of Atmospheric Radiance and Transmittance in Remote Sensing. Short Communication. Remote Sensing of Environment, 1983, vol. 13, pp. 89-92.

Deering, D. W. (1989): Field Measurements of Bidirectional Reflectance. Theory and Applications of Optical Remote Sensing, edt. Asrar, G., 1989, pp. 14-21.

Dozier, Jeff (1980): A Clear-Sky Spectral Solar Radiation Model for Snow-Covered Mountainous Terrain. Water Resources Research, 1980, vol. 16, no. 4, pp. 709-718.

Dozier, Jeff (1989): Remote Sensing of Snow in Visible and Near-Infrared Wavelengths. Theory and Applications of Optical Remote Sensing, edt. Asrar, G., 1989, pp. 527-547.

Fristrup, Børge (1970): Ny geografisk station i Grønland. Geografisk Tidsskrift, 1970, bind 69, pp. 192-203.

Hall & Martinec (1985): Remote Sensing of Ice and Snow. University Press, Cambridge.